arXiv:1703.06116v1 [math.NA] 13 Mar 2017

A SURFACE HOPPING GAUSSIAN BEAM METHOD FOR HIGH-DIMENSIONAL TRANSPORT SYSTEMS

ZHENNING CAI AND JIANFENG LU

Abstract. We propose a surface hopping Gaussian beam method to numerically solve a class of high frequency linear transport systems in high spatial dimensions, based on asymptotic analysis. The stochastic surface hopping is combined with Gaussian beam method to deal with the multiple characteristic directions of the transport system in high dimensions. The Monte Carlo nature of the proposed algorithm makes it easy for parallel implementations. We validate the performance of the algorithms for applications on the quantum-classical Liouville equations.

1. Introduction

In this paper we focus on the system of u_i^ϵ, $i = 1, \cdots, n$ with the following form:

$$\frac{\partial u_i^\epsilon(t,x)}{\partial t} + \alpha_i(t,x)^\top \nabla_x u_i^\epsilon(t,x) = \frac{\mathrm{i}}{\epsilon}\beta_i(t,x)u_i^\epsilon(t,x) + \sum_{j=1}^n \gamma_{ij}(t,x)u_j^\epsilon(t,x), \tag{1}$$

$$u_i^\epsilon(0,x) = v_i^\epsilon(x), \qquad i = 1, \cdots, n. \tag{2}$$

where ϵ is a small positive parameter and v_i^ϵ are initial conditions. For each i, the unknown $u_i^\epsilon(\cdot,\cdot)$ maps from $\mathbb{R}^+ \times \mathbb{R}^m$ to $\mathbb{C}$, where m is large so that this is a system in high spatial dimension. For each i, j, The coefficients $\alpha_i(\cdot,\cdot)$ maps from $\mathbb{R}^+ \times \mathbb{R}^m$ to $\mathbb{R}^m$, $\beta_i(\cdot,\cdot)$ maps from $\mathbb{R}^+ \times \mathbb{R}^m$ to $\mathbb{R}$, and $\gamma_{ij}(\cdot,\cdot)$ maps from $\mathbb{R}^+ \times \mathbb{R}^m$ to $\mathbb{C}$. If $n = 1$, the equation (1) becomes a linear transport equation with a stiff source term. When $n > 1$, the system consists of n such ingredients and they interact with each other through the second linear term on the right hand side. For simplicity, here we assume that all the coefficients $\alpha_i(\cdot,\cdot)$, $\beta_i(\cdot,\cdot)$ and $\gamma_{ij}(\cdot,\cdot)$ are smooth functions.

Systems with the form (1) arise in several application fields. In this work, we focus in particular on the quantum-classical Liouville equation (QCLE) [15, 24], which is a model for mixed quantum-classical dynamics (say for quantum systems consist of nuclei and electrons). The equations are derived through an adiabatic representation of the Hamiltonian and a partial Wigner transform of the von Neumann equation. As a result, the leading orders of the equation have the form (1), and the terms with α_i, β_i and γ_{ij} in (1) respectively represent the transport of particles, the phase oscillation, and the exchange between phases [11]. Numerical study of single and dual crossing examples in [11] shows that QCLE can accurately predict the population of each adiabatic states when comparing with the fully quantum results. We will come back to more details of QCLE in our numerical experiments. Another example of (1) worth mentioning is the multi-component transport equations [8, 7] with linear interactions with the form

$$\frac{\partial f_i(t,r,p)}{\partial t} = -\frac{\partial H_i(r,p)}{\partial p}\frac{\partial f_i(t,r,p)}{\partial r} + \frac{\partial H_i(r,p)}{\partial r}\frac{\partial f_i(t,r,p)}{\partial p} + \sum_{j=1}^n \left[\gamma_{j\to i} f_j(t,r,p) - \gamma_{i\to j} f_i(t,r,p)\right],$$

for $i = 1, \cdots, n$, where $f_i(t,r,p)$ and $H_i(r,p)$ are respectively the distribution function and the Hamiltonian for the ith component, and $\gamma_{i\to j}$ is the rate of change from the ith component to the jth component.

While vast research has been done in numerical schemes for advection-reaction systems in low spatial dimensions (see e.g., [13] for a review), the high dimensionality poses great challenges to conventional numerical schemes. In such cases, the grid-based methods become prohibitively expensive due to the curse of dimensionality, and we are therefore motivated to develop particle-type methods for the system.

This work is partially supported by the National Science Foundation under Grant Nos. DMS-1454939 and RNMS11-07444 (KI-Net). The authors would like to thank Giovanni Ciccotti for illuminating discussions.

Besides the high dimensionality, the fast oscillation of the solution due to the β term on the right hand side and perhaps the initial data poses additional challenge to the problem. Semiclassical methods are typically used to deal with such high frequency wave problems, such as the Gaussian beam method [10, 22, 9] and also more recently the method based on nonlinear geometric optics [5].

Let us focus on the Gaussian beam method. The basic idea is to first approximate the initial data of the equation with the superposition of many Gaussians with small variance, and then propogate each Gaussian as asymptotic solution to the equation, the solution is then given by the superposition of the Gaussians at a given time. The oscillation of the solution is naturally built into the Gaussian ansatz. For scalar equations ($n = 1$), the Gaussian beam method has been extensively studied, especially for the classical Liouville equation [19, 12, 27]. Such methods (including the nonlinear geometric optics method) however cannot be applied to systems as (1) due to the presence of the zeroth-order "γ-term", since this term may cause the number of the Gaussian beams to be multiplied by n at each time step, and eventually leads to an exponential increment of the Gaussian beams, which is obviously infeasible.

To avoid large amount of Gaussian beams, we consider using a Monte Carlo method to make it feasible. Thus, at each time step, we have only one Gaussian beam, but the Gaussian beam may contribute to any component of the solution randomly according to the γ-term. In particular, for the QCLE as mentioned earlier, the γ-term appears in the equation corresponding to the "surface hopping" of the trajectories [15, 11, 14], which corresponds to the random choice of the component. Such a perspective is widely used in understanding the quantum-classical dynamics, and it is often used to understand the fewest switches surface hopping algorithm for Schrödinger equations [26, 2]. The basic idea of the surface hopping method is to evolve trajectories on several "surfaces", and let the trajectories stochastically hop from one surface to another from time to time. This algorithm is mostly applied to the Schrödinger equation, and a recent paper by one of the authors [18] provides a mathematical understanding of the fewest switch surface hoppping algorithm [26]. The surface hopping method for the quantum-classical Liouville equation has been considered in [11, 20, 17, 16], while those methods are heuristically proposed without rigorous error control.

The main contribution of our work is a novel semiclassical approach that generalizes Gaussian beam method for systems like (1). We call the proposed method the *surface hopping Gaussian beam method*, as it combines the ideas of Gaussian beam method and surface hopping to solve (1). The algorithm allows each trajectory to be evolved independently, and thus its parallelization becomes trivial. In order to motivate the algorithm clearly, we first derive the Gaussian beam part and the surface hopping part of the algorithm independently, and then combine them together. The proposed method is verified both theoretically and numerically. This work also depicts the surface hopping in a clearer and more general sense, especially from the mathematical point of view.

In the remaining part of this paper, the proposed surface hopping Gaussian beam method is constructed in Section 2, where the Gaussian beam method and the surface hopping method are developed respectively in Section 2.1 and Section 2.2, and Section 2.3–2.5 describe and validate the whole algorithm with initial data processing. Numerical examples are given in Section 3. The whole paper is briefly summarized in Section 4.

2. Construction of the surface hopping Gaussian beam method

For simplicity, let us first assume that the initial data v_i^ϵ in (2) has the following form:

$$v_i^\epsilon(x) = G^\epsilon(M_0, N_0, X_0, P_0, S_0, A_0; x)\delta_{ii_0}, \qquad i = 1, \cdots, n, \tag{3}$$

where M_0 and N_0 are $m \times m$ real symmetric matrices, $X_0, P_0 \in \mathbb{R}^m$, $S_0 \in \mathbb{R}$, $A_0 \in \mathbb{C}$, and $i_0 \in \{1, \cdots, n\}$. The function G^ϵ is given by

$$G^\epsilon(M, N, X, P, S, A; x) = A \exp\left(-\frac{(x-X)^\top (M + \mathrm{i}N)(x-X)}{2\epsilon} + \frac{\mathrm{i}P^\top (x-X)}{\epsilon} + \mathrm{i}\frac{S}{\epsilon}\right). \tag{4}$$

Apparently G^ϵ defines a "Gaussian beam" with width $\sqrt{\epsilon}$, amplitude A, and center X. The matrix M is required to be positive definite so that the function decays to zero at infinity. General initial conditions will be represented as superposition of such Gaussian beams as discussed in Section 2.5.

To motivate the surface hopping Gaussian beam method, we will consider first the following two special cases of the system (1):

$$\frac{\partial u_i^\epsilon(t,x)}{\partial t} + \alpha_i(t,x)^\top \nabla_x u_i^\epsilon(t,x) = \frac{\mathrm{i}}{\epsilon}\beta_i(t,x)u_i^\epsilon(t,x) + \gamma_{ii}(t,x)u_i^\epsilon(t,x), \quad i = 1, \cdots, n, \tag{5}$$

and,

$$\frac{\partial u_i^\epsilon(t,x)}{\partial t} = \sum_{\substack{j=1 \\ j\neq i}}^{n} \gamma_{ij}(t,x)u_j^\epsilon(t,x), \quad i = 1, \cdots, n. \tag{6}$$

The system (5) is obtained by setting all the off-diagonal entries of the matrix (γ_{ij}) to be zero in (1), and the system (6) can be obtained by setting all the coefficients other than the off-diagonal entries of (γ_{ij}) to be zero. Note that (5) can be viewed as "diagonal terms" of (1), while (6) captures the "off-diagonal terms".

In the remainder of this section, we will first apply the Gaussian beam method to (5), and then apply the surface hopping method to (6). The fusion of these two parts follows thereafter, which eventually becomes a method solving the system (1) in the general case.

2.1. **The Gaussian beam method for the scalar equation.** The system (5) actually consists of n independent scalar equations for each u_i^ϵ, $i = 1, \cdots, n$. Since the initial condition v_i^ϵ is nonzero only if $i = i_0$, we have $u_i^\epsilon \equiv 0$ if $i \neq i_0$, and the system reduces to a single scalar equation with $i = i_0$ in (5). Here we recall the standard Gaussian beam method applying to the particular case (5).

In the Gaussian beam method, we take the ansatz

$$u_{i_0}^\epsilon(t,x) \approx U_{i_0}^\epsilon(t,x) = G^\epsilon(M(t), N(t), X(t), P(t), S(t), A(t); x). \tag{7}$$

By direct calculation, we get the derivatives appearing in (5) as

$$\begin{aligned}\frac{\partial U_{i_0}^\epsilon(t,x)}{\partial t} = \frac{1}{\epsilon}\Bigg[&(x-X(t))^\top[M(t)+\mathrm{i}N(t)]\frac{\mathrm{d}X(t)}{\mathrm{d}t} - \frac{1}{2}(x-X(t))^\top\left(\frac{\mathrm{d}M(t)}{\mathrm{d}t} + \mathrm{i}\frac{\mathrm{d}N(t)}{\mathrm{d}t}\right)(x-X(t)) \\ &+ \mathrm{i}(x-X(t))^\top\frac{\mathrm{d}P(t)}{\mathrm{d}t} - \mathrm{i}P(t)^\top\frac{\mathrm{d}X(t)}{\mathrm{d}t} + \mathrm{i}\frac{\mathrm{d}S(t)}{\mathrm{d}t} + \frac{\epsilon}{A(t)}\frac{\mathrm{d}A(t)}{\mathrm{d}t}\Bigg]U_{i_0}^\epsilon(t,x),\end{aligned} \tag{8}$$

$$\nabla_x U_{i_0}^\epsilon(t,x) = \frac{1}{\epsilon}\left[\mathrm{i}P(t) - M(t)(x-X(t)) - \mathrm{i}N(t)(x-X(t))\right]U_{i_0}^\epsilon(t,x). \tag{9}$$

Since

$$|x-X|^k G^\epsilon(M,N,X,P,S,A;x) \sim O(\epsilon^{k/2}), \qquad \forall k \in \mathbb{N}, \tag{10}$$

for a smooth function $f(t,x)$ independent of ϵ, we have the following approximation:

$$\begin{aligned}f(t,x)G^\epsilon(t;x) = \Bigg[&f(t,X(t)) + \Big(\nabla_x f(t,X(t))\Big)^\top(x-X(t)) \\ &+ \frac{1}{2}(x-X(t))^\top\nabla_x^2 f(t,X(t))(x-X(t))\Bigg]G^\epsilon(t;x) + O(\epsilon^{3/2}).\end{aligned} \tag{11}$$

Since we have already assumed the smoothness of $\alpha_{i_0}(t,x)$, $\beta_{i_0}(t,x)$ and $\gamma_{i_0 j}(t,x)$, the function $f(t,x)$ in (11) can be replaced by these coefficients and the equality still holds. Thus, by substituting (8) and (9) into (5), and applying the above result, we find that $U_{i_0}^\epsilon$ satisfies (5) up to a residual with relative L^∞ error $O(\epsilon^{1/2})$, if the functions $N(t)$, $X(t)$, $P(t)$, $S(t)$ and $A(t)$ fulfill the following equations obtained by matching the terms with the same orders of ϵ:

$$O(\epsilon^{-1}): \frac{\mathrm{d}S(t)}{\mathrm{d}t} + P(t)^\top\left(\alpha_{i_0}(t,X(t)) - \frac{\mathrm{d}X(t)}{\mathrm{d}t}\right) = \beta_{i_0}(t,X(t)),$$

$$O(\epsilon^{-\frac{1}{2}}): M(t)\left(\frac{\mathrm{d}X(t)}{\mathrm{d}t} - \alpha_{i_0}(t,X(t))\right) = 0,$$

$$\frac{\mathrm{d}P(t)}{\mathrm{d}t} + [\nabla_x\alpha_{i_0}(t,X(t))]^\top P(t) + N(t)\left(\frac{\mathrm{d}X(t)}{\mathrm{d}t} - \alpha_{i_0}(t,X(t))\right) = \nabla_x\beta_{i_0}(t,X(t)),$$

$$O(1): \mathrm{Re}\left(\frac{1}{A(t)}\frac{\mathrm{d}A(t)}{\mathrm{d}t}\right) - \frac{1}{\epsilon}(x-X(t))^\top\left[\frac{1}{2}\frac{\mathrm{d}M(t)}{\mathrm{d}t} + M(t)\nabla_x\alpha_{i_0}(t,X(t))\right](x-X(t)) = \mathrm{Re}\,\gamma_{i_0 i_0}(t,X(t)),$$

$$\mathrm{Im}\left(\frac{1}{A(t)}\frac{\mathrm{d}A(t)}{\mathrm{d}t}\right) - \frac{1}{\epsilon}(x-X(t))^\top\left[\frac{1}{2}\frac{\mathrm{d}N(t)}{\mathrm{d}t} - \frac{1}{2}\nabla_x^2(P(t)\cdot\alpha_{i_0})(t,X(t)) + N(t)\nabla_x\alpha_{i_0}(t,X(t))\right](x-X(t))$$
$$= \frac{1}{2}(x-X(t))^\top\nabla_x^2\beta_{i_0}(t,X(t))(x-X(t)) + \mathrm{Im}\,\gamma_{i_0i_0}(t,X(t)).$$

It is not difficult to find that the above equations hold if the parameters of G^ϵ evolve according to the following system of ODEs:

$$\begin{aligned}
&\frac{\mathrm{d}X(t)}{\mathrm{d}t} = \alpha_{i_0}(t,X(t)),\\
&\frac{\mathrm{d}S(t)}{\mathrm{d}t} = \beta_{i_0}(t,X(t)),\\
&\frac{\mathrm{d}P(t)}{\mathrm{d}t} = \nabla_x\beta_{i_0}(t,X(t)) - [\nabla_x\alpha_{i_0}(t,X(t))]^\top P(t),\\
&\frac{\mathrm{d}A(t)}{\mathrm{d}t} = \gamma_{i_0i_0}(t,X(t))A(t),\\
&\frac{\mathrm{d}M(t)}{\mathrm{d}t} = -M(t)\nabla_x\alpha_{i_0}(t,X(t)) - [\nabla_x\alpha_{i_0}(t,X(t))]^\top M(t),\\
&\frac{\mathrm{d}N(t)}{\mathrm{d}t} = \nabla_x^2(P(t)\cdot\alpha_{i_0})(t,X(t)) - \nabla_x^2\beta_{i_0}(t,X(t)) - N(t)\nabla_x\alpha_{i_0}(t,X(t)) - [\nabla_x\alpha_{i_0}(t,X(t))]^\top N(t).
\end{aligned} \tag{12}$$

The following proposition ensures that the matrix $M(t)$ is positive definite:

Proposition 1. *Suppose $B_1(t)$ and $B_2(t)$ are maps from $\mathbb{R}^+$ to $\mathbb{R}^{m\times m}$, and both matrix functions are bounded and piecewise continuous. Then the solution of*

$$\begin{aligned}
&\frac{\mathrm{d}M(t)}{\mathrm{d}t} = B_1(t) + M(t)B_2(t) + [B_2(t)]^\top M(t),\\
&M(0) = M_0 \in \mathbb{R}^{m\times m}
\end{aligned} \tag{13}$$

exists and is symmetric and positive definite for all $t > 0$ if the following two conditions hold:

- *M_0 is symmetric and positive definite;*
- *$B_1(t)$ is symmetric and positive semi-definite for all $t > 0$.*

The proof of the above proposition can be found in [6]. We have thus established the Gaussian beam method for (5). One only needs to solve the ordinary differential system (12) to get the approximation solution of (5). Since all the terms with orders higher than or equal to $O(\epsilon^{1/2})$ are dropped in the derivation of the method, the error of the Gaussian beam method is $O(\epsilon^{1/2})$, which can be made rigorous and we omit the details here.

2.2. **Surface hopping method for the ODE system.** Note that for each fixed x, equation (6) is a system of ODEs, while such ODEs can be solved easily by taking the exponent of the matrix coefficients, in this section, we propose an alternative stochastic algorithm for such equations. The reason is that the stochastic algorithm (the surface hopping algorithm) can be easily combined with the Gaussian beam, while it is impossible for the direct ODE solution as seen below.

Define the matrix functions $\Gamma(t,x) = (\tilde{\gamma}_{ij}(t,x))_{n\times n}$ and $\Theta(t,x) = (\Theta_{ij}(t,x))_{n\times n}$ as

$$\tilde{\gamma}_{ij}(t,x) = \begin{cases}\gamma_{ij}(t,x) & \text{if } i\neq j,\\ 0 & \text{if } i = j,\end{cases} \qquad \Theta(t,x) = \exp\left(\int_0^t \Gamma(s,x)\mathrm{d}s\right), \tag{14}$$

where the function $\exp(\cdot)$ means the matrix exponent. It is easy to see that the solution to (6) is

$$u_i^\epsilon(t,x) = \Theta_{ii_0}(t,x)v_{i_0}^\epsilon(x) = \Theta_{ii_0}(t,x)G^\epsilon(M_0,N_0,X_0,W_0,S_0,A_0;x), \qquad i = 1,\cdots,n. \tag{15}$$

This solution does not have a Gaussian shape in general due to the dependence of Θ_{ii_0} on x. To move forward, as we aim to combine this with the Gaussian beam method, we would like to find an approximation to the above solution with a Gaussian beam form. This can be easily achieved by defining

$$U_i^\epsilon(t,x) = \Theta_{ii_0}(t,X_0)v_{i_0}^\epsilon(x) = \Theta_{ii_0}(t,X_0)G^\epsilon(M_0,N_0,X_0,W_0,S_0,A_0;x), \qquad i = 1,\cdots,n. \tag{16}$$

Note that the argument of Θ has been replaced to X_0 above, which is the fixed center of the Gaussian. Using (10), we have that $U_i^\epsilon(t,x) - u_i^\epsilon(t,x) \sim O(\epsilon^{1/2})$. Thus U_i^ϵ approximates the solution of (6) with accuracy

$O(\epsilon^{1/2})$, which accords with the accuracy for the scalar equations in the last section. It is not difficult to find that U_i^ϵ is the solution of the following linear system:

$$\frac{\partial U_i^\epsilon(t,x)}{\partial t} = \sum_{\substack{j=1\\ j\neq i}}^{n} \gamma_{ij}(t, X_0) U_j^\epsilon(t,x), \quad i = 1, \cdots, n, \tag{17a}$$

$$U_i^\epsilon(0,x) = v_i^\epsilon(x) = G^\epsilon(M_0, N_0, X_0, W_0, S_0, A_0; x)\delta_{ii_0}, \quad i = 1, \cdots, n. \tag{17b}$$

While U_i^ϵ gives an approximate solution, the solution consists of a Gaussian for each surface $i = 1, \cdots, n$. This is undesirable, as if we combine this with the Gaussian beam method, each time step would then create multiple Gaussian beams for each Gaussian, which leads to exponential increase of the number of Gaussians as time proceeds, which is impractical as stated in the beginning of this section. To overcome this difficulty, below we will propose a stochastic representation to the solution of (17), which is the core of the surface hopping method. For conciseness of notation, we abbreviate $\gamma_{ij}(t, X_0)$ as $\gamma_{ij}(t)$ in the remainder of this section.

For the surface hopping method, we define a stochastic jump process

$$\ell = \{l_t : t \in \mathbb{R}^+\} \tag{18}$$

in the state space $\{1, \cdots, n\}$. We assume that the initial state is fixed as $l_0 = i_0$. If the solution of the equation can be formulated as

$$U_i^\epsilon(t,x) = \mathbb{E}[\mathcal{F}_i(\ell; t, x)], \qquad i = 1, \cdots, n \tag{19}$$

for some functionals $\mathcal{F}_i(\cdot;\cdot,\cdot)$, then U_i^ϵ can be numerically obtained by Monte Carlo sampling ℓ and taking the average of $\mathcal{F}_i(\ell; t, x)$. Before we determine the functionals $\mathcal{F}_i$, we would first like to give a clear definition of the jump process ℓ, and write out an explicit formula for the expectation $U_i^\epsilon(t,x)$.

Assume the process ℓ has state j at time t, and as $h \to 0$, we have

$$\mathbb{P}(l_{t+h} = i \mid l_t = j) = \delta_{ij} + \Omega_{ij}(t)h + o(h), \qquad i, j = 1, \cdots, n, \tag{20}$$

where the infinitesimal hopping probability $\Omega_{ij}(t)$ satisfies

$$\Omega_{ij}(t) \geqslant 0 \quad \text{if } i \neq j \qquad \text{and} \qquad \Omega_{jj}(t) = -\sum_{\substack{i=1\\ i\neq j}}^{n} \Omega_{ij}(t), \tag{21}$$

so that

$$\sum_{i=1}^{n} \mathbb{P}(l_{t+h} = i \mid l_t = j) = 1. \tag{22}$$

Let J_{t_1,t_2} be the number of jumps in the time interval (t_1, t_2) (so it is a random variable), and then $\mathbb{P}(J_{t_1,t_2} = 0)$ is the probability that no jump occurs in (t_1, t_2), which can be obtained from (20) as

$$\mathbb{P}(J_{t_1,t_2} = 0) = \lim_{h\to 0} \prod_{k=1}^{\lceil (t_2-t_1)/h \rceil} \mathbb{P}(l_{t_1+kh} = l_{t_1} \mid l_{t_1+(k-1)h} = l_{t_1}) = \exp\left(\int_{t_1}^{t_2} \Omega_{l_{t_1} l_{t_1}}(s)\,\mathrm{d}s\right). \tag{23}$$

Based on this, we can show that

$$\begin{aligned} \mathbb{E}[\mathcal{F}_i(\ell; t, x)] = &\sum_{K=0}^{+\infty} \sum_{\substack{i_1=1\\ i_1\neq i_0}}^{n} \cdots \sum_{\substack{i_K=1\\ i_K\neq i_{K-1}}}^{n} \\ &\times \int_0^t \int_0^{t_K} \cdots \int_0^{t_2} \mathcal{F}_i(\ell; t, x) \left(\prod_{k=1}^{K} \Omega_{i_k i_{k-1}}(t_k)\right) \exp\left(\int_0^t \Omega_{l_s l_s}(s)\,\mathrm{d}s\right) \mathrm{d}t_1 \cdots \mathrm{d}t_{K-1}\,\mathrm{d}t_K, \end{aligned} \tag{24}$$

where ℓ is a corresponding realization of the jump process (18) given $i_1, \cdots, i_K$ and $t_1, \cdots, t_K$ as follows:

$$l_s = i_k \quad \text{if} \quad s \in (t_k, t_{k+1}), \qquad k = 0, \cdots, K. \tag{25}$$

In (25), we take the convention that $t_0 = 0$ and $t_{K+1} = t$ for simplicity. The summations and integrals (24) shows that all possiblities of the jump process ℓ are taken into account when evaluating the expectation of

$\mathcal{F}_i$. The product term contributes to the K jumps, and the exponential term contributes to the "no-jump" part of the process as in (23). A detailed derivation of (24) can be found in the Appendix A.

Next, we just need to write the solution of the system (17) in the form of (24). To do this, we write U_i^ϵ as

$$U_i^\epsilon(t,x) = G^\epsilon(0;x)\delta_{ii_0} + \sum_{\substack{j_1=1\\ j_1\neq i}}^{n} \int_0^t \gamma_{ij_1}(t_1) U_{j_1}^\epsilon(t_1,x)\,\mathrm{d}t_1. \tag{26}$$

This equation is obtained simply by doing a time integration on both sides of (17a) over $[0,t]$, and it gives the integral form of (17). In order to get a series, we insert (26) into the right hand side of (26) itself, and get a new expression of U_i^ϵ:

(27)

$$\begin{aligned} U_i^\epsilon(t,x) &= G^\epsilon(0;x)\delta_{ii_0} + \sum_{\substack{j_1=1\\ j_1\neq i}}^{n} \int_0^t \gamma_{ij_1}(t_1) G^\epsilon(0;x)\delta_{j_1 i_0}\,\mathrm{d}t_1 + \sum_{\substack{j_1=1\\ j_1\neq i}}^{n}\sum_{\substack{j_2=1\\ j_2\neq j_1}}^{n} \int_0^t\int_0^{t_1} \gamma_{ij_1}(t_1)\gamma_{j_1j_2}(t_2) U_{j_2}^\epsilon(t_1,x)\,\mathrm{d}t_2\,\mathrm{d}t_1 \\ &= G^\epsilon(0;x)\delta_{ii_0} + \sum_{\substack{i_1=1\\ i_1\neq i_0}}^{n} \int_0^t \gamma_{i_1i_0}(t_1) G^\epsilon(0;x)\delta_{ii_1}\,\mathrm{d}t_1 + \sum_{\substack{j_1=1\\ j_1\neq i}}^{n}\sum_{\substack{j_2=1\\ j_2\neq j_1}}^{n} \int_0^t\int_0^{t_1} \gamma_{ij_1}(t_1)\gamma_{j_1j_2}(t_2) U_{j_2}^\epsilon(t_1,x)\,\mathrm{d}t_2\,\mathrm{d}t_1. \end{aligned}$$

By repeatedly inserting (26) into the newly obtained expression of U_i^ϵ and applying the following change of variables

(28)

$$\begin{aligned} &\sum_{\substack{j_1=1\\ j_1\neq i}}^{n}\sum_{\substack{j_2=1\\ j_2\neq j_1}}^{n}\cdots\sum_{\substack{j_K=1\\ j_K\neq j_{K-1}}}^{n} \int_0^t\int_0^{t_1}\cdots\int_0^{t_{K-1}} \gamma_{ij_1}(t_1)\gamma_{j_1j_2}(t_2)\cdots\gamma_{j_{K-1}j_K}(t_K) G^\epsilon(0;x)\delta_{j_K i_0}\,\mathrm{d}t_K\cdots\mathrm{d}t_2\,\mathrm{d}t_1 \\ = &\sum_{\substack{i_1=1\\ i_1\neq i_0}}^{n}\sum_{\substack{i_2=1\\ i_2\neq i_1}}^{n}\cdots\sum_{\substack{i_K=1\\ i_K\neq i_{K-1}}}^{n} \int_0^t\int_0^{t_K}\cdots\int_0^{t_2} \gamma_{i_Ki_{K-1}}(t_K)\gamma_{i_{K-1}i_{K-2}}(t_{K-1})\cdots\gamma_{i_1i_0}(t_1) G^\epsilon(0;x)\delta_{ii_K}\,\mathrm{d}t_1\cdots\mathrm{d}t_{K-1}\,\mathrm{d}t_K, \end{aligned}$$

we will eventually obtain the following series form of U_i^ϵ:

$$U_i^\epsilon(t,x) = \sum_{K=0}^{+\infty}\sum_{\substack{i_1=1\\ i_1\neq i_0}}^{n}\sum_{\substack{i_2=1\\ i_2\neq i_1}}^{n}\cdots\sum_{\substack{i_K=1\\ i_K\neq i_{K-1}}}^{n} \int_0^t\int_0^{t_K}\cdots\int_0^{t_2} \left(\prod_{k=1}^{K}\gamma_{i_ki_{k-1}}(t_k)\right) G^\epsilon(0;x)\delta_{ii_K}\,\mathrm{d}t_1\cdots\mathrm{d}t_{K-1}\,\mathrm{d}t_K. \tag{29}$$

Now comparing (29) with (24), one easily finds that (19) is fulfilled by setting

$$\mathcal{F}_i(\ell;t,x) = \exp\left(-\int_0^t \Omega_{l_sl_s}(s)\,\mathrm{d}s\right)\prod_{k=1}^{K}\frac{\gamma_{i_ki_{k-1}}(t_k)}{\Omega_{i_ki_{k-1}}(t_k)} G^\epsilon(0;x)\delta_{ii_K}. \tag{30}$$

Note that when $i=j$, Ω_{ij} is defined in (21), and therefore it remains only to choose the infinitesimal jump probabilities $\Omega_{ij}(t)$ for $i\neq j$. The choice is nonunique. In fact, any positive function independent of ϵ can be used. In our algorithm, we use

$$\Omega_{ij}(t) = |\gamma_{ij}(t)|, \qquad i,j=1,\cdots,n \quad \text{and} \quad i\neq j, \tag{31}$$

so that the hop does not change the magnitude of the amplitude of the Gaussian beam. Based on (30), we can define a function $\omega(t)$ as the solution of

$$\frac{\mathrm{d}\omega(t)}{\mathrm{d}t} = -\Omega_{l_tl_t}(t) + \mathrm{i}\frac{\mathrm{d}J_{0,t}}{\mathrm{d}t}\arg\gamma_{l_{t+}l_{t-}}(t) = \sum_{\substack{j=1\\ j\neq l_t}}^{m}|\gamma_{jl_t}(t)| + \mathrm{i}\frac{\mathrm{d}J_{0,t}}{\mathrm{d}t}\arg\gamma_{l_{t+}l_{t-}}(t), \qquad \omega(0)=0, \tag{32}$$

where l_{t-} (l_{t+}) denotes the left (right) limit of l_t at time t. Since $J_{0,t}$ is the number of jumps before time t, it is right continuous with left limits, and for a given jump process defined by (25), the derivative of $J_{0,t}$ is (in the distributional sense)

$$\frac{\mathrm{d}J_{0,t}}{\mathrm{d}t} = \sum_{k=1}^{K}\delta(t-t_k). \tag{33}$$

Therefore the solution of (32) is

$$\omega(t) = \exp\left(\sum_{\substack{j=1\\ j\neq l_t}}^{m} |\gamma_{jl_t}(t)|\right) \prod_{k=1}^{K} \frac{\gamma_{i_k i_{k-1}}(t_k)}{|\gamma_{i_k i_{k-1}}(t_k)|}, \tag{34}$$

and then we have

$$U_i^\epsilon(t,x) = \mathbb{E}[\exp(\omega(t)) G^\epsilon(0;x)\delta_{il_t}]. \tag{35}$$

By now, it is clear that the numerical method for the system (17) contains the following ingredients:

- Draw a number of realizations of the jump process ℓ according to the infinitesimal jump probability (21).
- For each trajectory, solve $\omega(t)$ along the trajectory from (32).
- Take the average of all trajectories as (35) to get U_i^ϵ.

Due to the "δ_{il_t}" in the final result (35), we see that at time t, the jump process l_t only contributes to the l_tth component of the solution. Therefore, this algorithm can be described as a Gaussian hopping between different surfaces while the jump in l_t occurs. When there is no hop and the Gaussian stays at the ith surface, the Gaussian just evolves by changing its amplitude gradually (the coefficient $\exp(\omega(t))$ in (35) is continuous when l_t is a constant), which looks like travelling along a predefined surface. At the same time, the Gaussian is counted into the ith component of the solution. However, when the Gaussian hops from the ith surface to the jth surface, it stops its contribution to the ith component and becomes a part of the solution of the jth component. Exactly at the time point of such a hop, the amplitude of the Gaussian has a sudden change due to the discontinuity in $J_{0,t}$. This is why the algorithm is called surface hopping method. As we will see in the next subsection, when combined with the Gaussian beam method, the surface hopping provides a way to solve the high dimensional transport system.

2.3. **The surface hopping Gaussian beam method.** We now combine the two methods introduced in the last two sections to construct a stochastic solver for the original system (1). A natural way of such combination is to use the algorithm described in Section 2.2 to define a jump process, and do the same to the Gaussian as in the surface hopping method when a hop occurs. When there is no hop, the Gaussian G^ϵ evolves as in the Gaussian beam method described in Section 2.1, and its amplitude changes as in Section 2.2. A simple way to interpret such an combination is to use the idea of the time splitting method, which solve equations (5) and (6) alternately. Note that in the beginning of Section 2.2, we freeze the coefficients at point X_0 since X_0 is the center of the Gaussian (see (17a)). Here, the Gaussian beam is moving around, and therefore when solving (6), it is natural to freeze the coefficient $|\gamma_{ij}(t,x)|$ at the center of the current Gaussian beam. At each time step, we need to generate a random number to determine whether the trajectory hops at the current time step. Below, we are going to carry out such an idea without explicitly using the time splitting, so that much less random numbers are needed in the implementation.

We define the jump process l_t as (20), while the infinitesimal jump probability (31) is modified as

$$\Omega_{ij}(t) = |\gamma_{ij}(t, X(t))|, \qquad i,j = 1,\cdots,n \quad \text{and} \quad i \neq j, \tag{36}$$

where $X(t)$ is the center of the Gaussian as in Section 2.1. For each l_t, we solve the following ordinary differential system:

$$
\begin{aligned}
&\frac{\mathrm{d}X(t)}{\mathrm{d}t} = \alpha_{l_t}(t, X(t)),\\
&\frac{\mathrm{d}S(t)}{\mathrm{d}t} = \beta_{l_t}(t, X(t)),\\
&\frac{\mathrm{d}P(t)}{\mathrm{d}t} = \nabla_x \beta_{l_t}(t, X(t)) - [\nabla_x \alpha_{l_t}(t, X(t))]^\top P(t),\\
&\frac{\mathrm{d}A(t)}{\mathrm{d}t} = \gamma_{l_t l_t}(t, X(t))A(t),\\
&\frac{\mathrm{d}M(t)}{\mathrm{d}t} = -M(t)\nabla_x \alpha_{l_t}(t, X(t)) - [\nabla_x \alpha_{l_t}(t, X(t))]^\top M(t),\\
&\frac{\mathrm{d}N(t)}{\mathrm{d}t} = \nabla_x^2 (P(t)\cdot \alpha_{l_t})(t, X(t)) - \nabla_x^2 \beta_{l_t}(t, X(t)) - N(t)\nabla_x \alpha_{l_t}(t, X(t)) - [\nabla_x \alpha_{l_t}(t, X(t))]^\top N(t),\\
&\frac{\mathrm{d}\omega(t)}{\mathrm{d}t} = \sum_{\substack{j=1\\ j\neq l_t}}^{m} |\gamma_{j l_t}(t, X(t))| + \mathrm{i}\frac{\mathrm{d}J_{0,t}}{\mathrm{d}t} \arg \gamma_{l_{t+} l_{t-}}(t, X(t)),
\end{aligned}
\tag{37}
$$

with initial conditions

$$
X(0) = X_0, \quad S(0) = S_0, \quad P(0) = W_0, \quad A(0) = A_0, \quad M(0) = M_0, \quad N(0) = N_0, \quad \omega(0) = 0. \tag{38}
$$

It is clear that the first six equations in (37) come from the Gaussian beam method, but the index i_0 in (12) is replaced by l_t in the above system, since the Gaussian should follow the "current" surface which has the index l_t. The last equation in (37) comes from the surface hopping method for the ordinary differential system. Inspired by (35), an approximate solution of (1) is expected to be

$$
U_i^\epsilon(t, x) = \mathbb{E}[\exp(\omega(t)) G^\epsilon(t; x)\delta_{i l_t}], \qquad i = 1, \cdots, n. \tag{39}
$$

Below we will verify that (39) satisfies (1) up to a residual $O(\epsilon^{1/2})$.

The derivation in Section 2.2 shows that (39) can be expanded as (29) with $G^\epsilon(0; x)$ replaced by $G^\epsilon(t; x)$. For simplicity, we can employ the definition (14) to replace $\gamma_{i_k i_{k-1}}$ by $\tilde{\gamma}_{i_k i_{k-1}}$ in (29) and remove the constraints $i_1 \neq i_0$, $i_2 \neq i_1$, $\cdots$, $i_K \neq i_{K-1}$ in the summations. Furthermore, we let $\tau_K = (t_1, t_2, \cdots, t_K)^\top$ and define

$$
S_t^K = \{\tau_K \mid 0 \leqslant t_1 \leqslant \cdots \leqslant t_K \leqslant t\}. \tag{40}
$$

Thus for any function $f(t, t_1, \cdots, t_K)$, one has

$$
\int_{S_t^K} f(t, \tau_K)\, \mathrm{d}\tau_K = \int_0^t \int_0^{t_K} \cdots \int_0^{t_2} f(t, t_1, \cdots, t_K)\, \mathrm{d}t_1 \cdots \mathrm{d}t_{K-1}\, \mathrm{d}t_K. \tag{41}
$$

Using these notations, we can rewrite U_i^ϵ in a much simpler way as

$$
U_i^\epsilon(t, x) = \sum_{K=0}^{+\infty} \sum_{i_1, \cdots, i_K = 1}^{n} \int_{S_t^K} \left(\prod_{k=1}^{K} \tilde{\gamma}_{i_k i_{k-1}}(t_k, X(t_k)) \right) G^\epsilon(t; x)\delta_{i i_K}\, \mathrm{d}\tau_K. \tag{42}
$$

Now we are going to take the time derivative of U_i^ϵ. Note that the first six equations in (37) form a closed subsystem, and in the right hand side of the subsystem, discontinuities exist only in the jump process. Therefore $G^\epsilon(t, x)$ is a continuous function, and for a fixed jump process l_t, we can use the result in Section 2.1 to get

$$
\frac{\partial G^\epsilon(t; x)}{\partial t} + \alpha_{l_t}(t, x)^\top \nabla_x G^\epsilon(t; x) = \left(\frac{\mathrm{i}}{\epsilon} \beta_{l_t}(t, x) + \gamma_{l_t l_t}(t, x) \right) G^\epsilon(t; x) + O(\epsilon^{\frac{1}{2}}). \tag{43}
$$

Using

$$
\frac{\mathrm{d}}{\mathrm{d}t} \int_{S_t^K} f(t, \tau_K)\, \mathrm{d}\tau_K = \int_{S_t^{K-1}} f(t, \tau_{K-1}, t)\, \mathrm{d}\tau_{K-1} + \int_{S_t^K} \partial_t f(t, \tau_K)\, \mathrm{d}\tau_K, \tag{44}
$$

we can take the time derivative of (42) and get

(45)
$$\frac{\partial U_i^\epsilon(t,x)}{\partial t} = \sum_{K=0}^{+\infty} \sum_{i_1,\cdots,i_K=1}^{n} \tilde{\gamma}_{i_K i_{K-1}}(t,X(t)) \int_{S_t^{K-1}} \left(\prod_{k=1}^{K-1} \tilde{\gamma}_{i_k i_{k-1}}(t_k, X(t_k)) \right) G^\epsilon(t;x)\delta_{ii_K}\, \mathrm{d}\tau_{K-1} +$$
$$+ \sum_{K=0}^{+\infty} \sum_{i_1,\cdots,i_K=1}^{n} \int_{S_t^K} \left(\prod_{k=1}^{K} \tilde{\gamma}_{i_k i_{k-1}}(t_k, X(t_k)) \right) \left[\left(\frac{\mathrm{i}}{\epsilon}\beta_{i_K}(t,x) + \gamma_{i_K i_K}(t,x) - \alpha_{i_K}(t,x)^\top \nabla_x \right) G^\epsilon(t;x) \right] \delta_{ii_K}\, \mathrm{d}\tau_K + O(\epsilon^{\frac{1}{2}}).$$

This equation shows that in (42), the derivative of the integrand provides the contribution on the current surface, while the derivative of the integral bounds provides the contribution from the surface hopping term. In detail, we can write the above equality as $\partial_t U_i^\epsilon = \mathrm{I} + \mathrm{II} + O(\epsilon^{\frac{1}{2}})$ and get

$$\begin{aligned}
\mathrm{I} &= \sum_{K=0}^{+\infty} \sum_{i_1,\cdots,i_{K-1}=1}^{n} \tilde{\gamma}_{ii_{K-1}}(t,X(t)) \int_{S_t^{K-1}} \left(\prod_{k=1}^{K-1} \tilde{\gamma}_{i_k i_{k-1}}(t_k, X(t_k)) \right) G^\epsilon(t;x)\, \mathrm{d}\tau_{K-1} \\
&= \sum_{K=0}^{+\infty} \sum_{i_1,\cdots,i_{K-1}=1}^{n} \tilde{\gamma}_{ii_{K-1}}(t,x) \int_{S_t^{K-1}} \left(\prod_{k=1}^{K-1} \tilde{\gamma}_{i_k i_{k-1}}(t_k, X(t_k)) \right) G^\epsilon(t;x)\, \mathrm{d}\tau_{K-1} + O(\epsilon^{\frac{1}{2}}) \\
&= \sum_{j=1}^{n} \sum_{K=0}^{+\infty} \sum_{i_1,\cdots,i_{K-1}=1}^{n} \tilde{\gamma}_{ij}(t,x) \int_{S_t^{K-1}} \left(\prod_{k=1}^{K-1} \tilde{\gamma}_{i_k i_{k-1}}(t_k, X(t_k)) \right) G^\epsilon(t;x)\delta_{ji_{K-1}}\, \mathrm{d}\tau_{K-1} + O(\epsilon^{\frac{1}{2}}) \\
&= \sum_{j=1}^{n} \tilde{\gamma}_{ij}(t,x) U_j^\epsilon(t,x) + O(\epsilon^{\frac{1}{2}}),
\end{aligned} \tag{46}$$

where (10) is used in the second equality. For II, it is obvious that

$$\mathrm{II} = \left(\frac{\mathrm{i}}{\epsilon}\beta_i(t,x) + \gamma_{ii}(t,x) - \alpha_i(t,x)^\top \nabla_x \right) U_i^\epsilon(t,x). \tag{47}$$

Adding (46) and (47), we conclude that $U_i^\epsilon(t,x)$ defined by (39) satisfies

$$\frac{\partial U_i^\epsilon(t,x)}{\partial t} + \alpha_i(t,x)^\top \nabla_x U_i^\epsilon(t,x) = \frac{\mathrm{i}}{\epsilon}\beta_i(t,x) U_i^\epsilon(t,x) + \sum_{j=1}^{n} \gamma_{ij}(t,x) U_i^\epsilon(t,x) + O(\epsilon^{\frac{1}{2}}), \tag{48}$$

and therefore is an approximate solution of (1).

The algorithm to obtain such an approximate solution U_i^ϵ is implied in (36)–(39), and it will be made more explicit in the next section. The equations (37) show that while the Gaussian beam is traveling along the surfaces, it changes not only the amplitude, but also its shape, center and oscillation frequency. Thus, most of the time, the Gaussian beam moves following a "trajectory" on a surface, and at several time points, it hops from one surface to another stochastically. The average of all the trajectories gives the solution of the system (1).

2.4. **Outline of the algorithm.** Based on the above derivation, we list the detailed steps of the algorithm in this section. Before that, we claim that the time of the first jump t_1 can be picked by generating a random number $Y \sim U(0,1)$, and solve

$$Y = 1 - \exp\left(\int_0^{t_1} \Omega_{i_0 i_0}(s)\, \mathrm{d}s \right) = 1 - \exp\left(- \int_0^{t_1} \sum_{k=1}^{n} |\tilde{\gamma}_{ki_0}(s, X(s))|\, \mathrm{d}s \right). \tag{49}$$

This can be observed from (23), which tells us that the probability $\mathbb{P}(t_1 < T)$ is $1 - \mathbb{P}(J_{0,T} = 0)$, and therefore $Y \sim U(0,1)$ if $Y = 1 - \mathbb{P}(J_{0,t_1} = 0)$. Since the right hand side of (49) is an increasing function of t_1, the solution is unique, and the equation can be solved while evolving the trajectory. Other jump times t_2, t_3, $\cdots$ can be similarly generated.

Now we are ready to state our algorithm. We assume that we want to obtain $U_i^\epsilon(T,x)$ for all $j = 1, \cdots, n$.

(1) Set $N_{\mathrm{traj}} \leftarrow 0$ and $U_j^\epsilon(T,x) \leftarrow 0$ for all $j = 1, \cdots, n$.
(2) Set $i \leftarrow i_0$, $t \leftarrow 0$, $\tilde{\omega} \leftarrow 0$, *flag* $\leftarrow$ *false*. Set the initial conditions (38). Generate a random number $Y \sim U(0,1)$.

(3) Select the time step Δt. Assume that no hops occurs in $(t, t+\Delta t)$, and solve $\omega(t+\Delta t)$ according to (37).
(4) If $\exp(\tilde{\omega} - \omega(t+\Delta t)) \leqslant 1 - Y$, then solve the equation of the jump time $\tilde{t}$

$$\exp(\tilde{\omega} - \omega(\tilde{t})) = 1 - Y$$

by interpolation of $\omega(t)$ in $[t, t+\Delta t]$, and set $\Delta t \leftarrow \tilde{t} - t$ and *flag* $\leftarrow$ *true*.
(5) Solve the whole system (37) by Δt with the assumption that no hops occurs in $(t, t+\Delta t)$. Set $t \leftarrow t + \Delta t$. If *flag* is *true*, then generate a random integer $j \in \{1, \cdots, n\} \backslash \{i\}$ from the probability mass function

$$f(j) = |\gamma_{ji}(t, X(t))| \Big/ \sum_{\substack{k=1 \\ k \neq i}}^{n} |\gamma_{ki}(t, X(t))|, \qquad j \in \{1, \cdots, n\} \backslash \{i\},$$

generate a new $Y \sim U(0,1)$, and set

$$\omega(t) \leftarrow \omega(t) + \mathrm{i} \arg \gamma_{ji}(t, X(t)), \qquad i \leftarrow j, \qquad \tilde{\omega} \leftarrow \omega(t), \qquad \textit{flag} \leftarrow \textit{false}.$$

(6) If $t < T$, return to step 3. If $t \geqslant T$, then set

$$U_i^\epsilon(T, x) \leftarrow U_i^\epsilon(T, x) + \exp(\omega(T)) G^\epsilon(T; x), \qquad N_{\mathrm{traj}} \leftarrow N_{\mathrm{traj}} + 1.$$

(7) If N_{traj} is large enough, then set $U_j^\epsilon(T, x) \leftarrow U_j^\epsilon(T, x)/N_{\mathrm{traj}}$ for all $j = 1, \cdots, n$ and stop. Otherwise, return to step 2.

In this algorithm, the jump process l_t is hidden in the parameter i. The boolean *flag* indicates whether the hopping occurs at the current time step. The parameter $\tilde{\omega}$ records the value of ω at the time of last jump, and thus according to (49), the equation in step 4 determines the time of the first jump since the last jump. When it is known that a hop occurs between t and $t + \Delta t$, we shrink the time step Δt such that $t + \Delta t$ is exactly the time point of the next jump. The surface hopping is applied at step 5. It is obvious that we don't need to generate a random number at every time step as in a naive time splitting method. In our implementation, the system (37) is solved with a third-order Runge-Kutta method in step 3 and 5.

Remark. The above method can also be used to solve the following extension of the system (1):

(50)
$$\frac{\partial u_i^\epsilon(t,x)}{\partial t} + \alpha_i(t,x)^\top \nabla_x u_i^\epsilon(t,x) = \frac{\mathrm{i}}{\epsilon} \beta_i(t,x) u_i^\epsilon(t,x) + \sum_{j=1}^n \gamma_{ij}(t,x) u_j^\epsilon(t,x) + \sum_{j=1}^n \nu_{ij}(t,x) \overline{u_j^\epsilon(t,x)}, \quad i = 1, \cdots, n.$$

To do this, one can define $w_i^\epsilon(t,x) = \overline{u_i^\epsilon(t,x)}$ and rewrite the system (50) as

$$\frac{\partial u_i^\epsilon(t,x)}{\partial t} + \alpha_i(t,x)^\top \nabla_x u_i^\epsilon(t,x) = \frac{\mathrm{i}}{\epsilon} \beta_i(t,x) u_i^\epsilon(t,x) + \sum_{j=1}^n \gamma_{ij}(t,x) u_j^\epsilon(t,x) + \sum_{j=1}^n \nu_{ij}(t,x) w_j^\epsilon(t,x), \quad i = 1, \cdots, n,$$

$$\frac{\partial w_i^\epsilon(t,x)}{\partial t} + \alpha_i(t,x)^\top \nabla_x w_i^\epsilon(t,x) = \frac{\mathrm{i}}{\epsilon} \overline{\beta_i(t,x)} w_i^\epsilon(t,x) + \sum_{j=1}^n \overline{\gamma_{ij}(t,x)} w_j^\epsilon(t,x) + \sum_{j=1}^n \overline{\nu_{ij}(t,x)} u_j^\epsilon(t,x), \quad i = 1, \cdots, n.$$

The above system again has the form of (1), and thus the algorithm can be applied. We can average the results of $u_i^\epsilon(t,x)$ and $\overline{w_i^\epsilon(t,x)}$ to get the final result. Due to the special relation between u_i^ϵ and w_i^ϵ, when implementing the algorithm, we do not need to double the number of unknowns. When a hop from a u_i^ϵ-surface to a w_j^ϵ-surface occurs, we just need to set

$$A(t) \leftarrow \overline{A(t)}, \quad S(t) \leftarrow -S(t), \quad P(t) \leftarrow -P(t), \quad N(t) \leftarrow -N(t), \quad \omega(t) \leftarrow \overline{\omega(t)} \tag{51}$$

after the hop, and then continue the algorithm as if the Gaussian beam is on the u_j^ϵ-surface. Thus w_i^ϵ does not appear in the algorithm, while (51) is a hidden switch between u and w.

2.5. **Algorithm for general initial data.** The above discussion is based on the initial condition (2), which is a single Gaussian beam. This algorithm can be naturally extended to more general case due to the linearity of the equations. Suppose the initial data can be written as

(52)
$$v_i^\epsilon(x) = \int_{\mathbb{R}^m}\int_{\mathbb{R}^m}\int_{\mathbb{R}^{m\times m}}\int_{\mathbb{R}^{m\times m}} f_i^\epsilon(M,N,X,P)G^\epsilon(M,N,X,P,S_i(M,N,X,P),A_i(M,N,X,P);x)\,\mathrm{d}M\,\mathrm{d}N\,\mathrm{d}X\,\mathrm{d}P$$

for every $i = 1,\cdots,n$. If $f_i^\epsilon(M,N,X,P)$ has a support with nonzero measure and is absolutely integrable, then we can select $f_i^\epsilon(M,N,X,P)$ and $A_i(M,N,X,P)$ appropriately such that $f_i^\epsilon(M,N,X,P)\geqslant 0$ and

$$\int_{\mathbb{R}^m}\int_{\mathbb{R}^m}\int_{\mathbb{R}^{m\times m}}\int_{\mathbb{R}^{m\times m}} f_i^\epsilon(M,N,X,P)\,\mathrm{d}M\,\mathrm{d}N\,\mathrm{d}X\,\mathrm{d}P = 1. \tag{53}$$

In detail, if the positivity of $f_i^\epsilon(M,N,X,P)$ or (53) is not satisfied, we can set

$$f_i^\epsilon(M,N,X,P) \leftarrow |f_i^\epsilon(M,N,X,P)|/C_i, \qquad A_i(M,N,X,P) \leftarrow C_i f_i^\epsilon(M,N,X,P)/|f_i^\epsilon(M,N,X,P)|, \tag{54}$$

where C_i is selected such that (53) can be fulfilled.

To solve the system (1) with initial conditions (52), we only need to sample the initial parameters of the Gaussian beam according to the density functions f_i^ϵ. Concretely speaking, let

$$\mathcal{I} = \{i \mid \operatorname{supp} v_i^\epsilon \neq \varnothing\}, \tag{55}$$

and then we just need to change step 2 to the following:

(2) Randomly pick i from $\mathcal{I}$. Draw a sample M_0, N_0, X_0, W_0 from $f_i^\epsilon(M,N,X,P)$ and set

$S_0 \leftarrow S_i(M_0,N_0,X_0,W_0)$, $\quad A_0 \leftarrow n_{\mathcal{I}} A_i(M_0,N_0,X_0,W_0)$, $\quad t \leftarrow 0$, $\quad \tilde{\omega} \leftarrow 0$, $\quad$ *flag* $\leftarrow$ *false*.

Generate a random number $Y \sim U(0,1)$.

Thus all the trajectories start from different surfaces and different positions. Here $n_{\mathcal{I}}$ is the number of elements in the set $\mathcal{I}$. It is multiplied to the initial amplitude A_0 since when selecting the initial surface, the probablity of picking any element from $\mathcal{I}$ is $1/n_{\mathcal{I}}$, which will be introduced as a factor to the solution when we calculate the expectation. The expectation of these Gaussian beams is the expectation of the system's approximate solutions with initial data sampled in the above step, which is just an approximate solution of the system (1) due to its linearity.

The initial value decomposition and its accuracy are also discussed in a number of papers. Some recent development includes [25, 21, 1].

3. Numerical examples

3.1. **An example without modelling error.** We first consider the following two-dimensional system:

$$\begin{aligned}
&\frac{\partial u_1^\epsilon}{\partial t} - (x_1+x_2+1)\frac{\partial u_1^\epsilon}{\partial x_1} - (2x_1-x_2-1)\frac{\partial u_1^\epsilon}{\partial x_2} = \frac{\mathrm{i}}{\epsilon}|x|^2 u_1^\epsilon - u_1^\epsilon + \frac{1}{2}u_2^\epsilon,\\
&\frac{\partial u_2^\epsilon}{\partial t} - \left(\frac{1}{2}x_1+x_2-1\right)\frac{\partial u_2^\epsilon}{\partial x_1} - \left(x_1-\frac{1}{2}x_2+1\right)\frac{\partial u_1^\epsilon}{\partial x_2} = \frac{\mathrm{i}}{\epsilon}(x_1+x_2)^2 u_2^\epsilon + \frac{2}{3}u_1^\epsilon - 2u_2^\epsilon,
\end{aligned} \tag{56}$$

with initial value

$$u_1^\epsilon(0,x) = \exp\left(-\frac{|x|^2}{2}\right), \qquad u_2^\epsilon(0,x) = 0. \tag{57}$$

In order to apply the Gaussian beam method, we write the initial value of u_1^ϵ as

$$u_1^\epsilon(0,x) = \int_{\mathbb{R}^2} f^\epsilon(X)\cdot\frac{1}{\epsilon}\exp\left(-\frac{|x-X|^2}{2\epsilon}\right)\mathrm{d}X, \tag{58}$$

where $f^\epsilon(X)$ is a normal distribution

$$f^\epsilon(X) = \frac{1}{2\pi(1-\epsilon)}\exp\left(-\frac{|X|^2}{2(1-\epsilon)}\right). \tag{59}$$

Thus the initial Gaussian beam can be obtained by drawing X from $f^\epsilon(X)$.

In this example, the coefficients α_i are linear in x, β_i are quadratic, and γ_{ij} are constants. Therefore the $O(\epsilon^{\frac{1}{2}})$ residuals in (43) and (46) vanish. Hence the expectation $U_i^\epsilon(t,x)$ of the surface hopping Gaussian beam method is the exact solution of (56). Since (56) does not have an explicit analytical solution, we solve

the system with a finite volume method and the result is used a reference solution. The scheme is third order in both time and space, and the mesh is uniform with grid size $\Delta x_1 = \Delta x_2 = 0.02$. Figure 1 shows the numerical results for $\epsilon = 0.1$ at $t = 0.5$, which are obtained with 100,000 trajectories. The isolines are almost identical to the reference solution, which indicates the feasibility of the surface hopping Gaussian beam method.

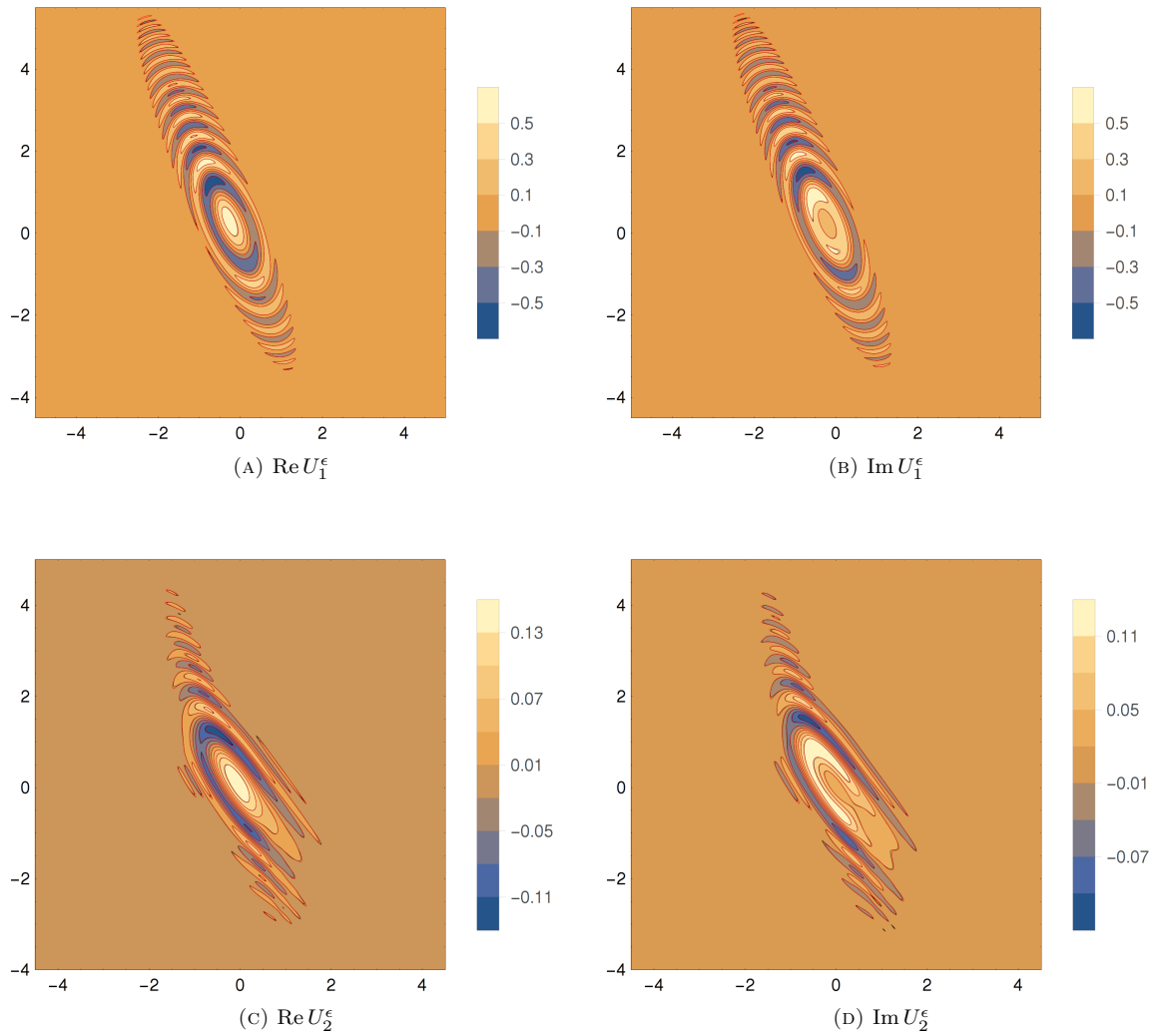

(A) $\operatorname{Re} U_1^\epsilon$ (B) $\operatorname{Im} U_1^\epsilon$

(C) $\operatorname{Re} U_2^\epsilon$ (D) $\operatorname{Im} U_2^\epsilon$

FIGURE 1. Comparison between the numerical result and the reference solution. The white lines show the contours of the reference solution, and the color shading and black lines (almost covered by the red lines) give the contours of the solution of the surface hopping Gaussian beam method.

Below we study the convergence of the surface hopping Gaussian beam method with respect to the number of trajectories N_{traj}. We run the above simulation with 100, 200, 400, 800, 1600, 3200, 6400 trajectories and compute the L^2 difference between the numerical solution and the reference solution. The result is plotted in Figure 2, where the case $\epsilon = 0.5$ is also included. The errors in the figure are obtained by averaging the erros of 100 runs in each case, and the error bars show the standard deviations. The figure clearly shows that both the error and its standard deviation decreases as $O(N_{\text{traj}}^{-1/2})$ when the number of trajectories increases, which agrees with the general property of stochastic numerical methods.

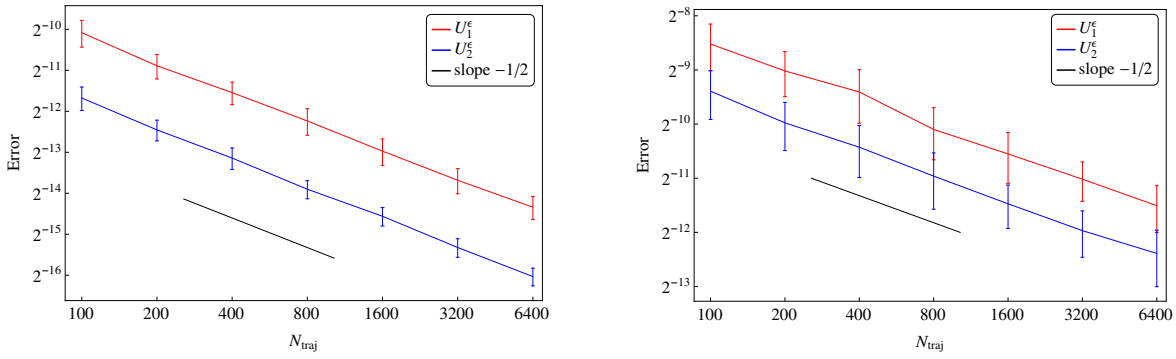

(A) $\epsilon = 0.1$ (B) $\epsilon = 0.5$

FIGURE 2. Log-log plot of the L^2 errors for U_1^ϵ and U_2^ϵ with different number of trajectories

3.2. **An example with nonlinear coefficients.** In this section, we consider the system

$$\begin{aligned}
&\frac{\partial u_1^\epsilon}{\partial t} - \sin(x_1+x_2)\frac{\partial u_1^\epsilon}{\partial x_1} - \cos(x_1-x_2)\frac{\partial u_1^\epsilon}{\partial x_2} = \frac{\mathrm{i}}{\epsilon}\sin(|x|^2)u_1^\epsilon - |x|^2(u_1^\epsilon - 5u_2^\epsilon),\\
&\frac{\partial u_2^\epsilon}{\partial t} - \sin(x_1-x_2)\frac{\partial u_2^\epsilon}{\partial x_1} - \cos(x_1+x_2)\frac{\partial u_2^\epsilon}{\partial x_2} = \frac{\mathrm{i}}{\epsilon}\cos(|x|^2)u_2^\epsilon - |x|^2\left(5u_1^\epsilon + \frac{1}{2}u_2^\epsilon\right),
\end{aligned} \tag{60}$$

with initial conditions

$$u_1^\epsilon(0,x) = \exp\left(-\frac{|x|^2}{2\epsilon}\right), \qquad u_2^\epsilon(0,x) = 0. \tag{61}$$

In this example, the coefficients are nonlinear in x, and therefore the $O(\epsilon^{\frac{1}{2}})$ residuals in (43) and (46) exist, which will lead to some discrepancy between u_i^ϵ and U_i^ϵ. Here we again use the finite volume solver to provide a reference solution, and the grid size is $\Delta x_1 = \Delta x_2 = 0.005$.

We consider four different values of ϵ. Figure 3–6 respectively show the results for $\epsilon = 0.08, 0.04, 0.02, 0.01$. All the simulations are performed using 10,000 trajectories. As expected, the solution spreads wider when ϵ increases, and the oscillation gets stronger when ϵ decreases. In all the cases, our method generates reasonable approximate solutoins, while it can still be observed from the figures that better approximation of the reference solution is obtained for smaller ϵ.

3.3. **Quantum-classical Liouville equation.** In this section, we consider the application of the surface hopping Gaussian beam method to the quantum-classical Liouville equation [24], which describes the composed system with heavy and light particles. The quantum-classical Liouville equation (QCLE) has exactly the form (50), and thus our algorithm can be directly applied. Here we study the two level system as in [4], and write the equations as

$$\begin{aligned}
\frac{\partial u_{11}^\epsilon(t,r,p)}{\partial t} &= -p\cdot\nabla_r u_{11}^\epsilon(t,r,p) + \nabla_r E_1(r)\cdot\nabla_p u_{11}^\epsilon(t,r,p) + [p\cdot\overline{d_{21}(r)}]u_{21}^\epsilon(t,r,p) + [p\cdot d_{21}(r)]\overline{u_{21}^\epsilon(t,r,p)},\\
\frac{\partial u_{22}^\epsilon(t,r,p)}{\partial t} &= -p\cdot\nabla_r u_{22}^\epsilon(t,r,p) + \nabla_r E_2(r)\cdot\nabla_p u_{11}^\epsilon(t,r,p) - [p\cdot\overline{d_{21}(r)}]u_{21}^\epsilon(t,r,p) - [p\cdot d_{21}(r)]\overline{u_{21}^\epsilon(t,r,p)},\\
\frac{\partial u_{21}^\epsilon(t,r,p)}{\partial t} &= -\frac{\mathrm{i}}{\epsilon}[E_2(r)-E_1(r)]u_{21}^\epsilon(t,r,p) - p\cdot\nabla_r u_{21}^\epsilon(t,r,p) + \frac{1}{2}\nabla_r[E_1(r)+E_2(r)]\cdot\nabla_p u_{21}^\epsilon(t,r,p)\\
&\quad + [p\cdot(d_{11}(r)-d_{22}(r))]u_{21}^\epsilon(t,r,p) - [p\cdot d_{21}(r)]u_{11}^\epsilon(t,r,p) + [p\cdot d_{21}(r)]u_{22}^\epsilon(t,r,p),
\end{aligned} \tag{62}$$

where $E_1(r), E_2(r) \in \mathbb{R}$ are adiabatic energy surfaces, $r \in \mathbb{R}^n$ and $p \in \mathbb{R}^n$ stand respectivly for the position and momentum, and $d_{ij}(r) \in \mathbb{R}^n$ is used to denote the first-order adiabatic operator. We refer the readers to [24, 4] for the derivation of the above equations, and here we just mention that $E_i(r)$ and $d_{ij}(r)$ can be derived from the potential energy matrix acting on the heavy particles $V(r) \in \mathbb{C}^{2\times 2}$. Assuming $V(r)$ to be

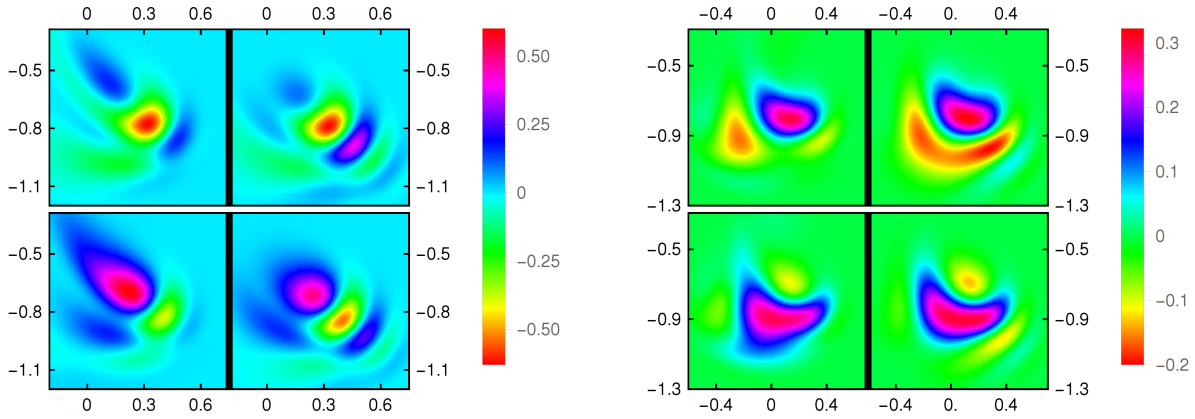

(A) U_1^ϵ and the reference solution (B) U_2^ϵ and the reference solution

FIGURE 3. Comparison between the numerical results and the reference solutions with $\epsilon = 0.08$. The upper half of the figure shows the real part of the solution, and the lower half shows the imaginary part. The results of the surface hopping Gaussian beam method are given to the right of the bold black bars, and the left parts are the reference solutions.

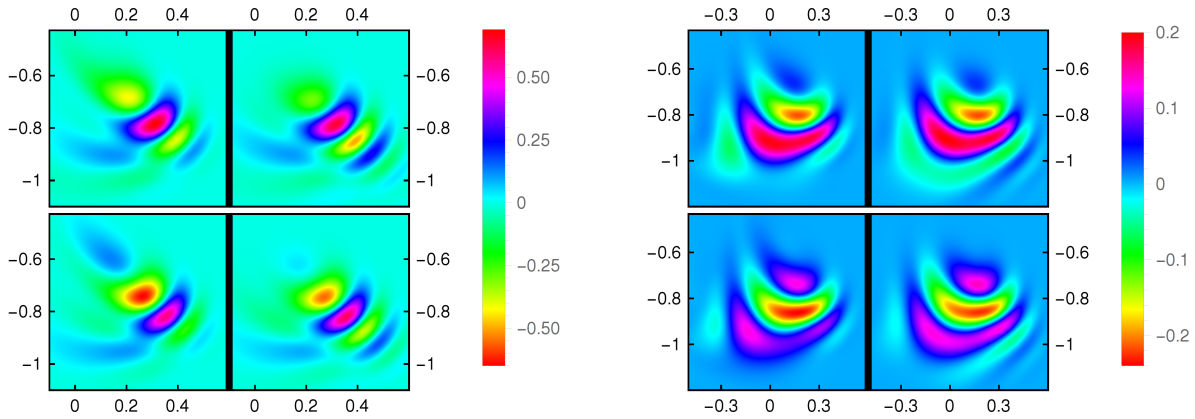

(A) U_1^ϵ and the reference solution (B) U_2^ϵ and the reference solution

FIGURE 4. Comparison between the numerical results and the reference solutions with $\epsilon = 0.04$. See Figure 3 for the details.

real and symmetric, we have

$$
\begin{aligned}
E_{1,2}(r) &= \frac{1}{2}[V_{11}(r) + V_{22}(r)] \pm \frac{1}{2}\sqrt{[V_{11}(r) - V_{22}(r)]^2 + 4V_{12}^2(r)}, \\
d_{21}(r) &= \frac{[V_{11}(r) - V_{22}(r)]\nabla_r V_{12}(r) - V_{12}(r)\nabla_r[V_{11}(r) - V_{22}(r)]}{[V_{11}(r) - V_{22}(r)]^2 + 4V_{12}^2(r)}, \quad d_{11}(r) = d_{22}(r) = 0.
\end{aligned} \tag{63}
$$

The equations (62) are slightly different from the more conventional QCLE derived in [15, 11]. The system (62) can be considered as the simplified version of the quantum-classical Liouville equations, where a momentum-jump term is absent. The simplification yields a $O(\epsilon)$ approximation to the quantum-classical expectation values of physical quantities [24]. We refer the readers to [11, 23, 3] for the comparisons of the two models.

Below we will present two examples to test our method.

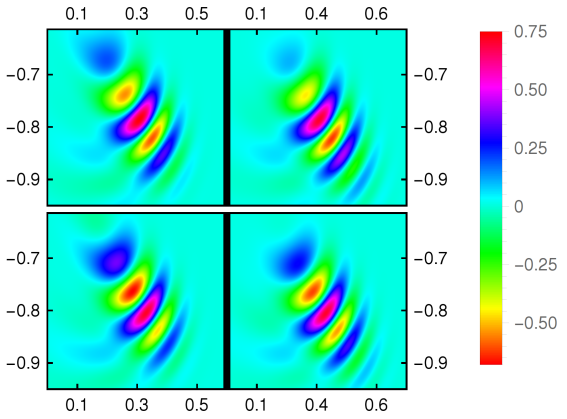

(A) U_1^ϵ and the reference solution

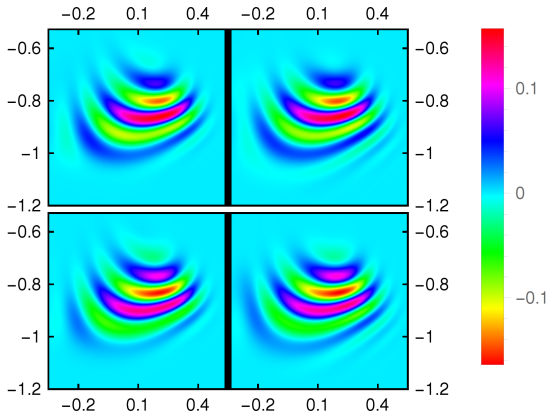

(B) U_2^ϵ and the reference solution

FIGURE 5. Comparison between the numerical results and the reference solutions with $\epsilon = 0.02$. See Figure 3 for the details.

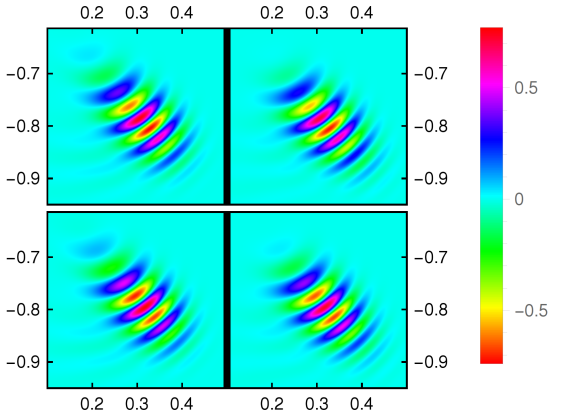

(A) U_1^ϵ and the reference solution

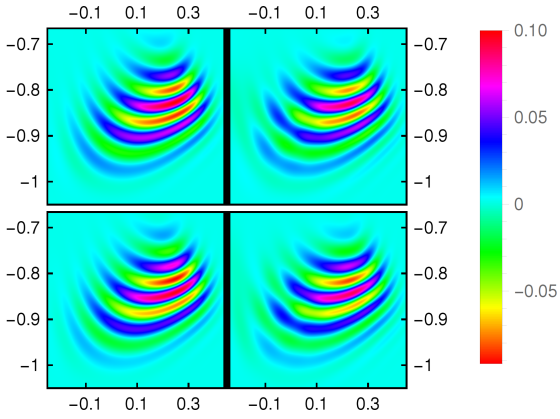

(B) U_2^ϵ and the reference solution

FIGURE 6. Comparison between the numerical results and the reference solutions with $\epsilon = 0.01$. See Figure 3 for the details.

3.3.1. *Extended coupling with reflection.* This example is from one of Tully's examples in [26]. The number of dimensions $n = 1$, and the matrix $V(r)$ is given as

$$V(r) = \begin{pmatrix} V_{11}(r) & V_{12}(r) \\ V_{12}(r) & V_{22}(r) \end{pmatrix} = F^\delta(r) \begin{pmatrix} \frac{1}{20} & \frac{1}{10}\left(\arctan(2r) + \frac{\pi}{2}\right) \\ \frac{1}{10}\left(\arctan(2r) + \frac{\pi}{2}\right) & -\frac{1}{20} \end{pmatrix}, \tag{64}$$

where $F^\delta(r) = \frac{1}{\pi}\left(\arctan(100r) + \frac{\pi}{2} + \delta\right)$. Here we choose $\delta = 5\epsilon$ and the initial condition

$$u_{11}^\epsilon(0,x) = u_{12}^\epsilon(0,x) = 0, \quad u_{22}^\epsilon(0,x) = \frac{1}{\sqrt{32\pi\epsilon}} \exp\left(-\frac{(r-r_0)^2}{\epsilon} - \frac{(p-p_0)^2}{\epsilon}\right), \tag{65}$$

and the initial position and momentum are set to be $r_0 = -1.5$ and $p_0 = 1.5$. Three cases $\epsilon = 1/16, 1/32, 1/64$ are considered, and in these cases, the energy surfaces $E_{1,2}(r)$ and the function $d_{21}(r)$ are plotted in Figure 7. From (62), one can find that $E_{1,2}(r)$ describes the "shape" of the surfaces, and $d_{21}(r)$ determines the probability of the surface hopping. In this example, $d_{21}(r)$ is indepedent of ϵ. If $r > 1.5$, there are hardly any hops between surfaces.

Due to the space limitations, we only plot figures for u_{11}^ϵ and u_{22}^ϵ. Figure 8–10 show the comparison with the reference solutions. In all cases, 10,000 trajectories are used and the figures show the solutions at $t = 2$.

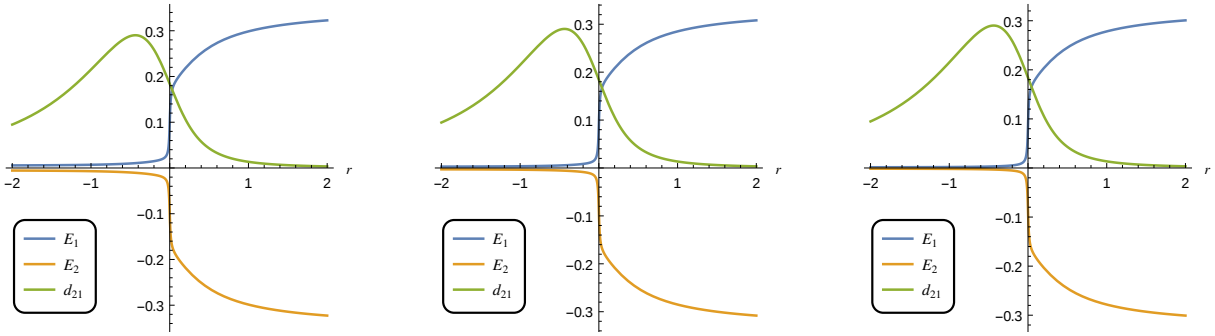

(A) $\epsilon = 1/16$ (B) $\epsilon = 1/32$ (C) $\epsilon = 1/64$

FIGURE 7. Funtions $E_1(r)$, $E_2(r)$ and $d_{21}(r)$ for various ϵ

We again observe that better results are obtained for small ϵ. Figure 11 gives a sample of the trajectory in the phase space (r, p), which is extracted from a test run for $\epsilon = 1/32$. When $r < 0$, both $E_1(r)$ and $E_2(r)$ are flat, and thus there is very little change in the momentum p. By zooming in, we can still see that the momentum is increasing slowly until the hop occurs. The first hop brings the trajectory onto the u^ϵ_{21} surface, where the momentum does not change since $E_1(r) + E_2(r)$ is zero. The second hop almost occurs at the point with highest hopping probability (see Figure 7). Since $E_1(r)$ is increasing, the momentum starts to drop at this hop. When crossing the point $r = 0$, the momentum has the fastest decrease. The last hop occurs near $r = 0$, and the momentum again stays as a constant from then on. Later, since r keeps increasing, the hopping probability goes lower, no more hops exist in the trajectory.

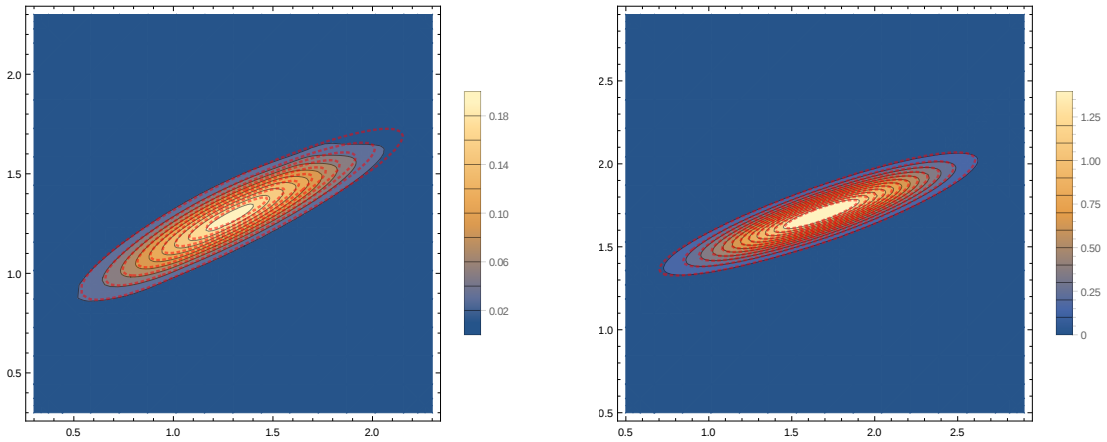

(A) U^ϵ_{11} and the reference solution (B) U^ϵ_{22} and the reference solution

FIGURE 8. Comparison between the numerical results (color shading and black contour lines) and the reference solutions (red dotted contour lines) for $\epsilon = 1/16$.

3.3.2. *Single crossing.* This example is a repetition of the example in [24, 11] with our method. We again consider the one-dimensional case $x, p \in \mathbb{R}$, and the diabatic potential energy matrix is

$$V(r) = \begin{pmatrix} r^2 & 1/10 \\ 1/10 & 1/r \end{pmatrix}. \tag{66}$$

Thus we have the potential energy $E_{1,2}(r)$, effective potential energy $\frac{1}{2}[E_1(r) + E_2(r)]$ and the nonadiabatic coupling coefficient $d_{21}(r)$ as in Figure 12. The initial value is

$$u^\epsilon_{11}(0, r, p) = \sqrt{\frac{2}{\pi\epsilon}} \exp\left(-\frac{(r - r_0)^2}{2\epsilon} - \frac{2(p - p_0)^2}{\epsilon}\right), \qquad u^\epsilon_{21}(0, r, p) = u^\epsilon_{22}(0, r, p) = 0. \tag{67}$$

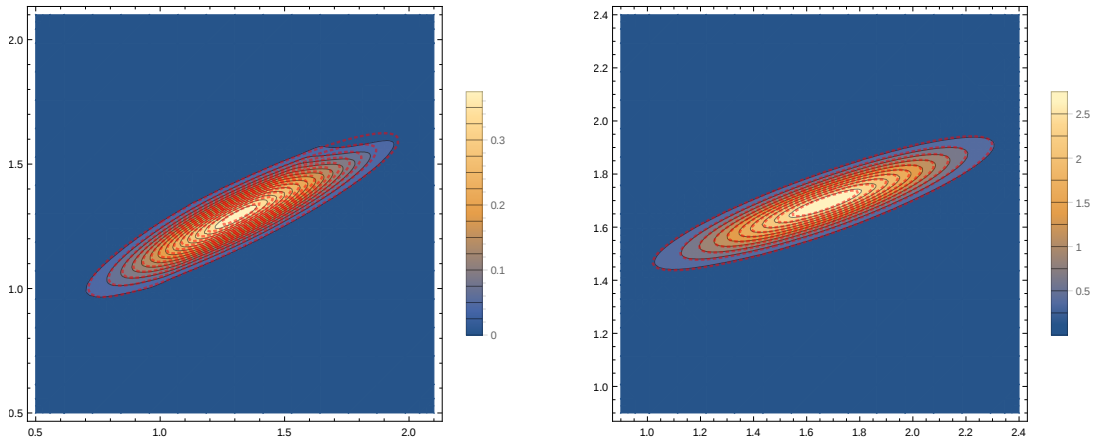

(A) U_{11}^{ϵ} and the reference solution (B) U_{22}^{ϵ} and the reference solution

FIGURE 9. Comparison between the numerical results (color shading and black contour lines) and the reference solutions (red dotted contour lines) for $\epsilon = 1/32$.

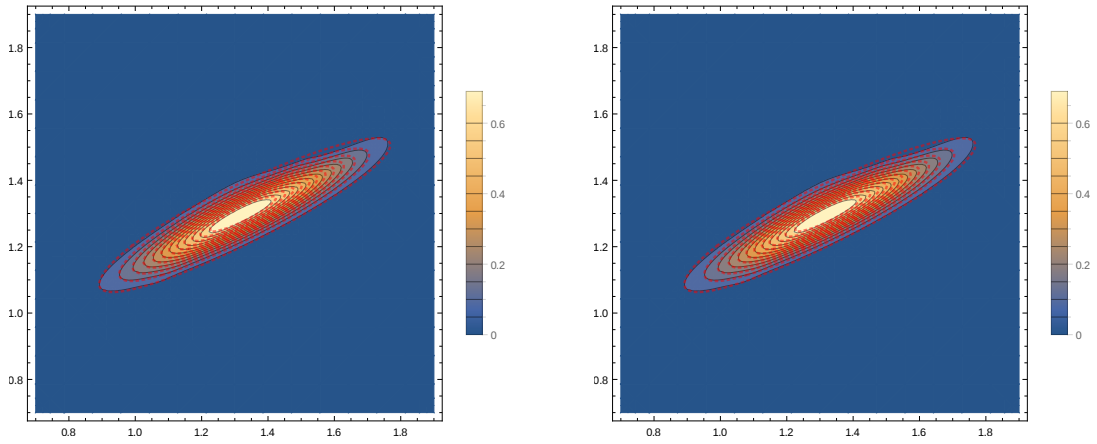

(A) U_{11}^{ϵ} and the reference solution (B) U_{22}^{ϵ} and the reference solution

FIGURE 10. Comparison between the numerical results (color shading and black contour lines) and the reference solutions (red dotted contour lines) for $\epsilon = 1/64$.

Following the method in [27], we write the initial value as

(68)
$$u_{11}^{\epsilon}(0,r,p) = \int_{\mathbb{R}}\int_{\mathbb{R}}\int_{\mathbb{R}}\int_{\mathbb{R}} f(r_1',p_1',r_2',p_2')A(r_1',p_1',r_2',p_2')\times \exp\left(-\frac{r^2+p^2}{\epsilon} - \frac{\mathrm{i}[p(r_1'-r_2') - r(p_1'-p_2')]}{\epsilon} + \frac{\mathrm{i}(p_1'-p_2')(r_1'+r_2')}{2\epsilon}\right) \mathrm{d}r_1'\,\mathrm{d}p_1'\,\mathrm{d}r_2'\,\mathrm{d}p_2',$$

where

(69)
$$f(r_1',p_1',r_2',p_2') = \frac{1}{18(\pi\epsilon)^2}\exp\left(-\frac{(r_1'-r_0)^2+(r_2'-r_0)^2}{6\epsilon} - \frac{(p_1'-p_0)^2+(p_2'-p_0)^2}{3\epsilon}\right),$$

(70)
$$A(r_1',p_1',r_2',p_2') = \frac{6}{\sqrt{\pi\epsilon}}\exp\left(\frac{\mathrm{i}(p_1'-p_0)(2r_1'+r_0)}{3\epsilon} - \frac{\mathrm{i}(p_2'-p_0)(2r_2'+r_0)}{3\epsilon}\right).$$

Thus the initial condition can be set by drawing r_1', p_1', r_2' and p_2' from (69).

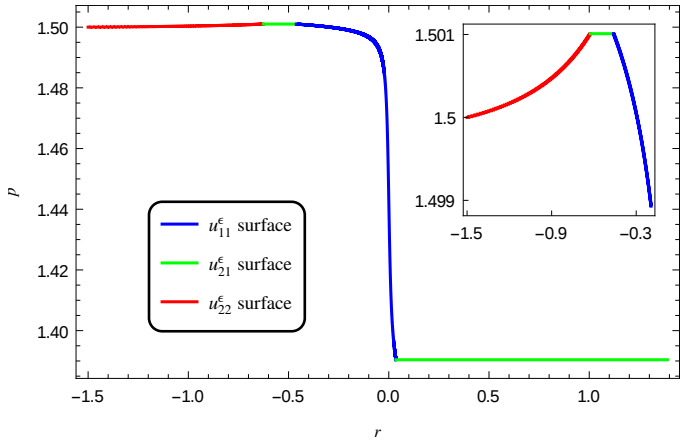

FIGURE 11. A sample trajectory with three surface hops

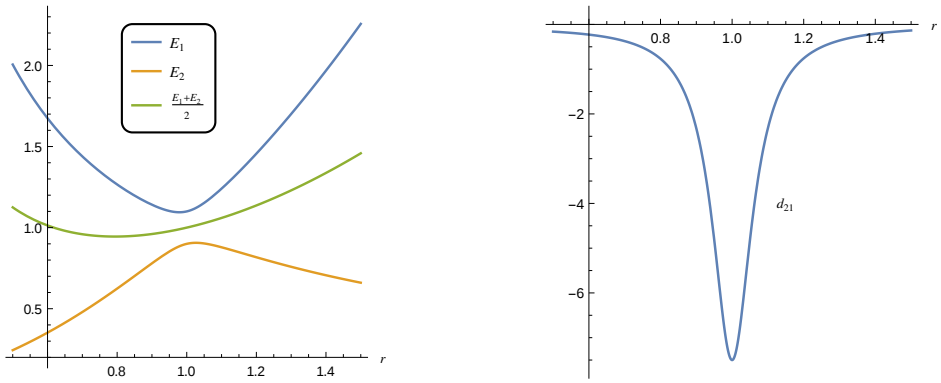

(A) Potential energies (B) Nonadiabatic coupling

FIGURE 12. Potential energies and nonadiabatic coupling for the single-crossing example

In our experiment, we follow [24, 11] and choose $r_0 = 0.4$, $p_0 = 1$ and $\epsilon = 0.01$. Figure 13 gives the numerical solution of U^ϵ_{11} and U^ϵ_{22} using 2,000,000 trajectories at $t = 0.5$. Unlike the last example, the solution no longer has a Gaussian shape after evolution. Our method can still well capture the structure of the solution both qualitatively and quantitatively. Using this as a reference solution, we measure the error of the numerical results for different numbers of trajectories, which are plotted in Figure 14. The errors are again obtained by averaging of 100 runs in each case. The half-order of convergence is still observed.

4. Summary

We presented a stochastic numerical method for a type of linear hyperbolic equations with stiff non-coupling source terms and non-stiff coupling source terms. The algorithm combines the Gaussian beam method and the surface hopping method. Similar as [18], this work establishes a surface hopping method based on a solid mathematical foundation, and therefore gives a better understanding of the surface hopping in a general setting. As an algorithm, it is very efficient for initial data with small variance, and works well with the parallelism. As elementary application on the quantum-classical dynamics has been shown, and it can be expected that the algorithm is capable of solving systems with a large number of particles (corresponding to higher spatial dimension), which will be explored in the future.

Appendix A. Derivation of the expectation

Here we present the derivation of the formula (24). Define $F(t; T_1, \cdots, T_K; i_0, i_1, \cdots, i_K)$ as the probability that ℓ jumps K times in $[0, t)$, and the kth jump occurs in $[0, T_k]$ and is from i_{k-1} to i_k (therefore $i_{k-1} \neq i_k$

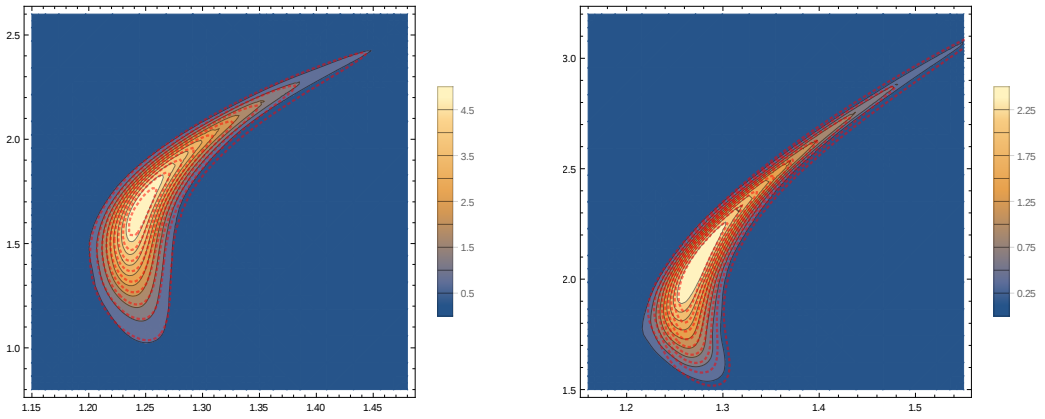

(A) U^ϵ_{11} and the reference solution (B) U^ϵ_{22} and the reference solution

FIGURE 13. Comparison between the numerical results (color shading and black contour lines) and the reference solutions (red dotted contour lines) for the single-crossing example.

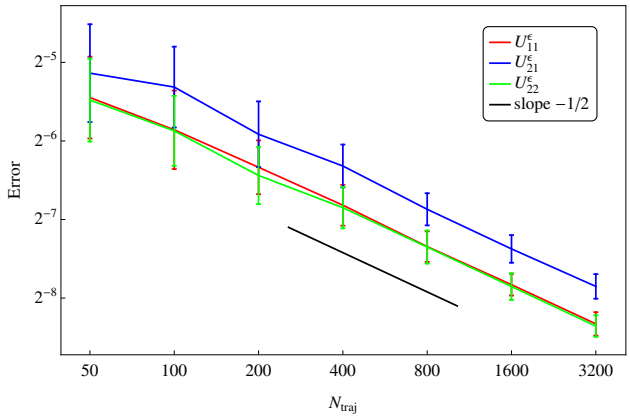

FIGURE 14. L^2-error for different numbers of trajectories

for every $k = 1, \cdots, K$). Obviously $F(t;;) = \mathbb{P}(J_{0,t} = 0)$, and we have

(71)
$$F(t; T_1, \cdots, T_K; i_0, \cdots, i_K) = \int_0^{\min(t,T_K)} F(t_K; T_1, \cdots, T_{K-1}; i_0, \cdots, i_{K-1}) \Omega_{i_{K-1} i_K}(t_K) \mathbb{P}(J_{t_K,t} = 0)\, \mathrm{d}t_K,$$

where t_K means the time of the Kth jump. The recursion relation (71) leads to

(72)
$$F(t; T_1, \cdots, T_K; i_0, \cdots, i_K) = \int_0^{\min(t,T_K)} \int_0^{\min(t_K,T_{k-1})} \cdots \int_0^{\min(t_2,T_1)} \left(\prod_{k=1}^{K} \Omega_{i_{k-1} i_k}(t_k) \right) \left(\prod_{k=0}^{K} \mathbb{P}(J_{t_k,t_{k+1}} = 0) \right) \mathrm{d}t_1 \cdots \mathrm{d}t_{K-1}\, \mathrm{d}t_K,$$

where $t_0 = 0$ and $t_{K+1} = t$. This formula clearly shows that given t and $i_0, \cdots, i_K$, the conditional probability density that the kth jump occurs at t_k is

(73)
$$\rho(t_1, \cdots, t_K \mid t; i_0, \cdots, i_K) = \begin{cases} 0, & \text{if } t_{k+1} < t_k \text{ for any } k = 0, \cdots, K, \\ \dfrac{1}{F(t; i_0, \cdots, i_K)} \left(\displaystyle\prod_{k=1}^{K} \Omega_{i_{k-1} i_k}(t_k) \right) \exp\left(\displaystyle\int_0^t \Omega_{l_s l_s}(s)\, \mathrm{d}s \right), & \text{otherwise,} \end{cases}$$

where $F(t;i_0,\cdots,i_K) := F(t;t,\cdots,t;i_0,\cdots,i_K)$ and l_s is the jump process defined in (25). Consequently, the expectation (19) can be written as

(74)

$$\begin{aligned}
&\mathbb{E}[\mathcal{F}_i(\ell;t,x)] \\
&= \sum_{K=0}^{+\infty} \sum_{\substack{i_1=1 \\ i_1\neq i_0}}^{n} \cdots \sum_{\substack{i_K=1 \\ i_K\neq i_{K-1}}}^{n} \int_0^{+\infty} \cdots \int_0^{+\infty} \mathcal{F}_i(\ell;t,x)\rho(t_1,\cdots,t_K \mid t;i_0,\cdots,i_K)F(t;i_0,\cdots,i_K)\,\mathrm{d}t_1\cdots\mathrm{d}t_K \\
&= \sum_{K=0}^{+\infty} \sum_{\substack{i_1=1 \\ i_1\neq i_0}}^{n} \cdots \sum_{\substack{i_K=1 \\ i_K\neq i_{K-1}}}^{n} \int_0^{t} \int_0^{t_K} \cdots \int_0^{t_2} \mathcal{F}_i(\ell;t,x) \left(\prod_{k=1}^{K} \Omega_{i_k i_{k-1}}(t_k)\right) \exp\left(\int_0^t \Omega_{l_s l_s}(s)\,\mathrm{d}s\right) \mathrm{d}t_1\cdots\mathrm{d}t_{K-1}\,\mathrm{d}t_K.
\end{aligned}$$

Here ℓ is the jump process defined by (25). This result is identical to (24).

References

1. G. Ariel, B. Engquist, N. Tanushev, and R. Tsai, *Gaussian beam decomposition of high frequency wave fields using expectation-maximization*, J. Comput. Phys. **230** (2011), no. 6, 2303–2321.
2. M. Barbatti, *Nonadiabatic dynamics with trajectory surface hopping method*, WIREs comput. Mol. Sci. **1** (2011), no. 4, 620–633.
3. Z. Cai and J. Lu, In preparation.
4. L. Chai, S. Jin, Q. Li, and O. Morandi, *A multi-band semiclassical model for surface hopping quantum dynamics*, Multiscale Model. Simul. **13** (2015), no. 1, 205–230.
5. N. Crouseilles, S. Jin, and M. Lemou, *Nonlinear geometric optics method based multi-scale mumerical schemes for highly-oscillatory transport equations*, arXiv:1605.09676 (2016).
6. L. Dieci and T. Eirola, *Positive definiteness in the numerical solution of Riccati differential equations*, Numerische Mathematik **67** (1994), no. 3, 303–313.
7. W. Dou, A. Nitzan, and J. E. Subotnik, *Frictional effects near a metal surface*, J. Chem. Phys. **143** (2015), no. 5, 054103.
8. F. Elste, G. Weick, C. Timm, and F. von Oppen, *Current-induced conformational switching in single-molecule junctions*, Appl. Phys. A **93** (2008), no. 2, 345–354.
9. G. A. Hagedorn, *Raising and lowering operators for semiclassical wave packets*, Comm. Pure Appl. Math. **50** (1997), no. 4, 323–379.
10. E. J. Heller, *Frozen Gaussians: A very simple semiclassical approximation*, J. Chem. Phys. **75** (1981), no. 6, 2923–2931.
11. I. Horenko, C. Salzmann, B. Schmidt, and C. Schütte, *Quantum-classical Liouville approach to molecular dynamics: Surface hopping Gaussian phase-space packets*, J. Chem. Phys. **117** (2002), no. 24, 11075–11088.
12. I. Horenko, B. Schmidt, and C. Schütte, *Multidimensional classical Liouville dynamics with quantum initial conditions*, J. Chem. Phys. **117** (2002), no. 10, 4643–4650.
13. W. Hundsdorfer and J. Verwer, *Numerical solution of time-dependent advection-diffusion-reaction equations*, Computational Mathematics, vol. 33, Springer, 2003.
14. R. Kapral, *Surface hopping from the perspective of quantum-classical Liouville dynamics*, Chem. Phys. **481** (2016), 77–83.
15. R. Kapral and G. Ciccotti, *Mixed quantum-classical dynamics*, J. Chem. Phys. **110** (1999), no. 18, 8919–8929.
16. A. Kelly and T. E. Markland, *Efficient and accurate surface hopping for long time nonadiabatic quantum dynamics*, J. Chem. Phys. **139** (2013), no. 1, 014104.
17. D. Mac Kernan, G. Ciccotti, and R. Kapral, *Trotter-based simulation of quantum-classical dynamics*, J. Phys. Chem. B **112** (2008), no. 2, 424–432.
18. J. Lu and Z. Zhou, *Frozen Gaussian approximation with surface hopping for mixed quantum-classical dynamics: A mathematical justification of fewest switches surface hopping algorithms*, `http://arxiv.org/abs/1602.06459`.
19. J. Ma, D. Hsu, and J. E. Straub, *Approximate solution of the classical Liouville equation using gaussian phase packet dynamics: Application to enhanced equilibrium averaging and global optimization*, J. Chem. Phys. **99** (1993), no. 5, 4024–4035.
20. D. MacKernan, R. Kapral, and G. Ciccotti, *Sequential short-time propagation of quantum-classical dynamics*, J. Phys.: Condens. Matter **14** (2002), no. 40, 9069–9076.
21. J. Qian and L. Ying, *Fast multiscale Gaussian wavepacket transforms and multiscale Gaussian beams for the wave equation*, Multiscale Model. Simul. **8** (2010), no. 5, 1803–1837.
22. J. Ralston, *Gaussian beams and the propagation of singularities*, Studies in Partial Differential Equations, Studies in mathematics, vol. 23, Mathematical Association of America, 1982, pp. 206–248.
23. I. G. Ryabinkin, C.-Y. Hsieh, R. Kapral, and A. F. Izmaylov, *Analysis of geometric phase effects in the quantum-classical Liouville formalism*, J. Chem. Phys. **140** (2014), no. 8, 084104.
24. C. Schütte, *Partial Wigner transforms and the quantum-classical Liouville equation*, Tech. Report SC-99-10, Konrad-Zuse-Center, 1999.
25. N. M. Tanushev, *Superpositions and higher order Gaussian beams*, Commun. Math. Sci. **6** (2008), no. 2, 449–475.
26. J. C. Tully, *Molecular dynamics with electronic transitions*, J. Chem. Phys. **93** (1990), no. 2, 1061–1071.

27. D. Yin, M. Tang, and S. Jin, *The Gaussian beam method for the Wigner equation with discontinuous potentials*, Inv. Prob. Imag. **7** (2013), no. 3, 1051–1074.

(Zhenning Cai) Department of Mathematics, National University of Singapore, Level 4, Block S17, 10 Lower Kent Ridge Road, Singapore 119076
E-mail address: matcz@nus.edu.sg

(Jianfeng Lu) Department of Mathematics, Department of Physics, Department of Chemistry, Duke University, Box 90320, Durham NC 27708, USA
E-mail address: jianfeng@math.duke.edu